

Stress Distribution in Soil under Action of Paraplow Ripper

Dzhaviger Eskhozhin¹, Sayakhat Nukeshev¹, Kairat Eskhozhin¹, Dimitar Karaivanov²

¹ Engineering Faculty, S. Seyfullin Kazakh Agro Technical University, 62 Zhenis Ave., Astana 100011, Kazakhstan

² Department of Applied Mechanics, University of Chemical Technology and Metallurgy, 8 Kl. Ohridski Blvd., Sofia 1756, Bulgaria, dipekabg@yahoo.com

Abstract: This article presents theoretical examination of interaction between paraplow ripper and soil based on linear mechanics theory. Stresses in soil layers and nature of their distribution are considered to be the main indicators of their interaction. Parabolic equations describing the distribution of normal and shearing stresses in soil were derived. Their numerical and graphical analysis allows solving the problem of working bodies balancing on the tillage tool's frame.

[Eskhozhin D, Nukeshev S, Eskhozhin K, Karaivanov D. **Stress Distribution in Soil under Action of Paraplow Ripper.** *Life Sci J* 2014;11(2s):20-24]. (ISSN:1097-8135). <http://www.lifesciencesite.com>. 5

Keywords: Normal stresses; paraplow ripper; shearing stresses; soil

1. Introduction

Soil is the primary source of food production for the population and raw materials for the processing industry. Its efficiency depends on the extent and effectiveness of the impact on it by working bodies of tillage machines and tools. Working bodies of tillage machines interacting with soil as a solid body transform it into different state. Currently, most publications in the area of mechanics of a solid body deformation concern to a certain extent the problem of different kinds of destruction. The destruction in solid mechanics means macroscopic discontinuity of the body as a result of exposure to the external environment and in particular the working parts of agricultural machines. It is clear that the fracture behavior will also be determined by the stress-strain state of the interacting systems (Broek, 1980; Morozov, Zernin 1990; Slepyan, 1990; Pluvinage, 1993). One of the key indicators of their interaction is the stresses in the soil layers under the influence of working bodies and their distribution (Eskhozhin, 2003). However, despite the large number of research papers on the interaction of working bodies with soil, the nature and distribution of the stresses in soil under the influence of various deformers, received insufficient attention (Freud, Clifton, 1974; Williams, 1975; Reidel, Rice, 1980; Reidel, 1987; Freud, 1990; Jun, Xing, 1995; Ferjani at al., 2011; Carrere, Martinez, 2013; Dewangan at al., 2013; Gao, Zhan, 2013; Ghosh, 2013). Meanwhile, its magnitude, depth and distribution distance in soil strongly affect the quality of soil tillage.

2. Material and Methods

This article presents theoretical study of interaction between soil and paraplow ripper which was developed specially for compact and alkaline

soils of Northern and Central Kazakhstan, characteristic for about 70% of all agricultural lands (Nukeshev, 2011). The study is based on the research of J. Boussinesq and V. Kirpichev, who in 1885 and 1930 correspondingly when considering the action of a concentrated force on the half-plastic medium have adopted the assumption of radial stress distribution on the basis of Newton's law of universal gravitation and proved the adequacy of the obtained solutions to describe the stress condition. This assumption states that radial normal stresses are directly proportional to the cosine of the angle between them and the direction of the applied force and inversely proportional to the square of the distance from the examined point of the semispace to the point of application of the concentrated force (Vyalov, 1978).

3. Results

Figure 1 shows the interaction between the paraplow ripper and soil semispace, constrained by O-y axis. Take into consideration the point M of the semispace, whose position is determined by radius R of the hemisphere and the angles β and ζ . The impact of the paraplow ripper on spherical semispace can be substituted by concentrated force \bar{P} with its projection P on the direction of movement.

According to the linear mechanics theory of soil, at every elementary spherical site S_R of a hemispherical surface the action of a concentrated force causes normal radial stress. According to J. Boussinesq's assumption it is equal to:

$$\sigma_R = A \frac{\cos \beta \cdot \cos \zeta}{R^2}, \quad (1)$$

where R is radius of the hemisphere; β is the angle between the direction of the applied force and the

radial stress; ζ is the angle between the direction of the applied force and the x-O-y plane, A is an unknown factor.

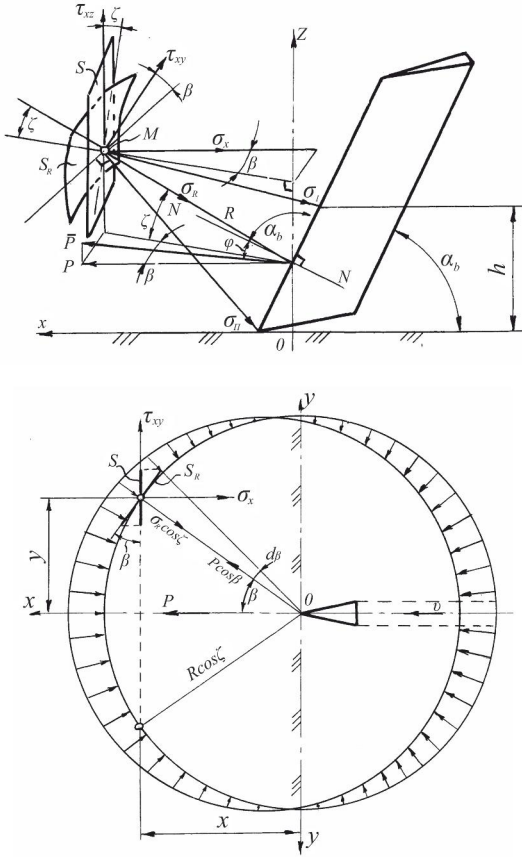


Figure 1. Determination of stress in soil under the effect of paraplow ripper

From (1) it is clear that the radial stress equals zero at $\beta = \frac{\pi}{2}$ at the constraining subspace of the semisphere and is maximal at $\beta = 0$ in the direction of the paraplow ripper's action.

Obviously, the sum of normal stresses must be balanced by the acting force of the paraplow ripper:

$$\int_0^{\pi/2} \sigma_R \cdot \cos \zeta \cdot \cos \beta \cdot dS_R = P \cdot \quad (2)$$

Elementary spherical site is equal to:

$$dS_R = 2\pi \cdot R \cdot h_s = 2\pi \cdot R \cdot R \cdot d\beta \cdot \sin \beta,$$

where h_s is the height of spherical segment. Therefore, taking consideration of (1), equation (2) changes to

$$2A \cdot \pi \cdot \cos^2 \zeta \int_0^{\pi/2} \cos^2 \beta \cdot \sin \beta \cdot d\beta = P \cdot$$

$$\text{With } \zeta = \frac{\pi}{2} - \alpha_b,$$

where α_b is the angle of paraplow ripper mounting; φ is the soil and metal friction angle.

It is clear that ζ does not depend on β , so it is taken out of the integral.

Integration of the last expression leads to the following:

$$\begin{aligned} 2A \cdot \pi \cdot \cos^2 \zeta \int_0^{\pi/2} \cos^2 \beta \cdot d(-\cos \beta) &= \\ = 2A \cdot \pi \cdot \cos^2 \zeta \left[-\frac{\cos^3 \beta}{3} \right]_0^{\pi/2} &= P \\ P - \frac{2}{3} A \times \pi \times \cos^2 \zeta &= 0 \end{aligned} \quad (3)$$

The unknown factor can be derived from (3):

$$A = \frac{3P}{2\pi} \cdot \frac{1}{\cos^2 \zeta} \quad (4)$$

Taking into consideration equation (4), radial normal stress (1) takes the following form:

$$\sigma_R = \frac{3P}{2\pi \cdot R^2} \cdot \frac{\cos \beta}{\cos \zeta} \quad (5)$$

Analyzing the distribution of stresses in the ground soil will be more convenient if the radial stress applied to the spherical site S_R is expanded on three directions applied to elementary site S , perpendicular to the direction of motion. The angles between the elementary sites equal to β in the horizontal plane and ζ in the vertical plane. Directions of expansion: the first is perpendicular to the elementary site, the second and the third lie in the elementary site and are directed to y and z. In this case, we have:

$$\begin{aligned} \sigma_x &= \sigma_R \cdot \cos \zeta \cdot \cos \beta \\ \tau_{xy} &= \sigma_R \cdot \cos \zeta \cdot \sin \beta \\ \tau_{xz} &= \sigma_R \cdot \sin \zeta \end{aligned} \quad (6)$$

Considering (5):

$$\begin{aligned} \sigma_x &= \frac{3P}{2\pi \cdot R^2} \cdot \cos^2 \beta \\ \tau_{xy} &= \frac{3P}{2\pi \cdot R^2} \cdot \cos \beta \cdot \sin \beta \\ \tau_{xz} &= \frac{3P}{2\pi \cdot R^2} \cdot \frac{\cos \beta}{\cos \zeta} \sin \zeta \end{aligned} \quad (7)$$

Expressing the trigonometric functions in equation (7) through the coordinates of the point M:

$$\sin \zeta = \frac{z}{R}; \quad \cos \zeta = \left[1 - \left(\frac{z}{R} \right)^2 \right]^{1/2}; \quad (8)$$

$$\cos \beta = \frac{x}{R} \cdot \frac{1}{\left[1 - \left(\frac{z}{R} \right)^2 \right]^{1/2}};$$

$$\sin \beta = \frac{y}{R} \cdot \frac{1}{\left[1 - \left(\frac{z}{R} \right)^2 \right]^{1/2}},$$

where:

$$R = \sqrt{x^2 + y^2 + z^2} = x \left[1 + \left(\frac{y}{x} \right)^2 + \left(\frac{z}{x} \right)^2 \right]^{1/2}.$$

Substituting the values of trigonometric functions of (8) in (7):

$$\sigma_x = \frac{3P}{2\pi \cdot R^2} \cdot \frac{x^2}{R^2} \cdot \frac{1}{\left[1 - \left(\frac{z}{R} \right)^2 \right]}; \quad (9)$$

$$\tau_{xy} = \frac{3P}{2\pi \cdot R^2} \cdot \frac{x \cdot y}{R^2} \cdot \frac{1}{\left[1 - \left(\frac{z}{R} \right)^2 \right]};$$

$$\tau_{xz} = \frac{3P}{2\pi \cdot R^2} \cdot \frac{x \cdot z}{R^2} \times \frac{1}{\left[1 - \left(\frac{z}{R} \right)^2 \right]},$$

where:

$$\frac{1}{R^2 \left[1 - \left(\frac{z}{R} \right)^2 \right]} = \frac{1}{x^2 \left[1 + \left(\frac{y}{x} \right)^2 \right]} \quad (10)$$

With regard to (10), the system (9) becomes:

$$\sigma_x = \frac{P}{R^2} \cdot \frac{3}{2\pi \left[1 + \left(\frac{y}{x} \right)^2 \right]}; \quad (11)$$

$$\tau_{xy} = \frac{P \cdot y}{R^2 \cdot x} \times \frac{3}{2\pi \left[1 + \left(\frac{y}{x} \right)^2 \right]};$$

$$\tau_{xz} = \frac{P \cdot z}{R^2 \cdot x} \times \frac{3}{2\pi \left[1 + \left(\frac{y}{x} \right)^2 \right]}.$$

In the system of equations (11) the second factors depend only on the ratio of x and y coordinates. We denote them:

$$k = \frac{3}{2\pi \left[1 + \left(\frac{y}{x} \right)^2 \right]} \quad (12)$$

In this case, compressing normal stresses σ_x and shear shifting stresses τ_{xy} and τ_{xz} take the form:

$$\sigma_x = k \cdot P \cdot \frac{1}{R^2}$$

$$\tau_{xy} = k \cdot P \cdot \frac{y}{R^2 \cdot x}$$

$$\tau_{xz} = k \cdot P \cdot \frac{z}{R^2 \cdot x}$$

The resulting concentrated force of the paraplow ripper's knife acting on the soil-ground semispace equals to (Figure 1):

$$\bar{P} = N \cdot \tan \varphi, \quad (14)$$

where N is the normal force of the paraplow ripper's knife on soil.

Projection of this force on the movement direction equals to:

$$P = \bar{P} \cdot \sin(\alpha_b + \varphi). \quad (15)$$

In such a way the system of equations describing the stress state of the soil (13) takes the following final form:

$$\sigma_x = k \cdot \bar{P} \cdot \sin(\alpha_b + \varphi) \cdot \frac{1}{R^2}$$

$$\tau_{xy} = k \cdot \bar{P} \cdot \sin(\alpha_b + \varphi) \cdot \frac{y}{R^2 \cdot x} \quad (16)$$

$$\tau_{xz} = k \cdot \bar{P} \cdot \sin(\alpha_b + \varphi) \cdot \frac{z}{R^2 \cdot x}$$

4. Discussions

The resulting parabolic equations on the distribution of stress in soil under the action of paraplow ripper allow to solve the problem of the angle of its installation and arrangement in the longitudinal and vertical planes. For illustration of the stress state of the soil under the action of paraplow ripper, stress calculations are conducted using equations (12) and (16) and the Table 1.

The following values are assumed for calculations:

$P = 9810$ N – the value of paraplow ripper's force applied to soil;

$\alpha_b = 65^\circ$ – paraplow ripper installation angle;

$\varphi = 25^\circ$ – the angle of soil and metal friction.

In this case $\sin(\alpha_b + \varphi) = 1$ in (16).

According to calculations the graphs of compressive and shear stress were drawn in Figure 2. The figure shows that the compressive stress in the direction of the external force, with the increase of distance from its point of application is significantly reduced. For example, at the depth of 1 cm compressive stress is 48 MPa, at the depth of 2 cm it is 12 MPa, at the depth of 10 cm it is 0.48 MPa, and at the depth of 20 cm it is 0.12 MPa, (Figure 2, curve $\sigma_x (y = 0)$).

Table 1. Stress distribution in soil under the action of paraplow ripper

x, y, z cm	R (y = 0, z = 0) cm	y, z cm	$\frac{y}{x}$ (x = 10) cm	k (y = 0)	k (x = 10)	σ_x MPa (y = 0) (z = 0) R = x	σ_x MPa (x = 10) (y = 0 ÷ 20) R ² =x ² +y ²	τ_{xy} MPa (x = 10) (y = 0 ÷ 20) R ² =x ² +y ²	τ_{xz} MPa (x = 10) (z = 0 ÷ 20) R ² =x ² +z ²
0	0	0	∞	0,48	0,48	∞	0,48	0	0
2	2	2	0,2	0,48	0,46	12,0	0,44	0,088	0,088
4	4	4	0,4	0,48	0,41	3,0	0,35	0,14	0,14
6	6	6	0,6	0,48	0,35	1,33	0,26	0,15	0,15
8	8	8	0,8	0,48	0,29	0,75	0,18	0,14	0,14
10	10	10	1,0	0,48	0,24	0,48	0,12	0,12	0,12
12	12	12	1,2	0,48	0,196	0,33	0,08	0,096	0,096
14	14	14	1,4	0,48	0,16	0,24	0,054	0,075	0,075
16	16	16	1,6	0,48	0,13	0,18	0,03	0,058	0,058
18	18	18	1,8	0,48	0,113	0,15	0,026	0,048	0,048
20	20	20	2,0	0,48	0,096	0,12	0,02	0,038	0,038

A similar situation occurs at the points remote from the line of action of external force. Thus, the compressive stress $\sigma_x(x=10)$ at the depth of 10 cm, along the line of action of the external force is 0.48 MPa, and when increasing distance to the side by 10 cm (y = 10) decreases down to 0.12 MPa, and by 20 cm it is 0.019 MPa. Shear stress along the line of action of an external force, as it is known, equal to zero, only compressive stresses are active. With increasing distance from the central direction shear stress increases and at the distance of about 6-8 cm reach their maximum – 0.154 MPa (Figure 2, curve $\tau_{xy}(x=10)$). When moving further it decreases, and at the distance of 20 cm it equals to 0.038 MPa.

A similar situation is typical for shear stress in the transverse vertical plane τ_{xz} . As can be seen from the illustration, the shear stress decreases more rapidly in the longitudinal direction along the working body. Thus, at a distance of 20 cm in the movement direction and along the side, the shear stress in the latter case is more than doubled compared to the first and equals respectively to 0.022 and 0.011 MPa.

The nature of the change of shear stresses in the soil in the longitude and vertical directions are similar to the previous one.

Given above stress distribution in the soil, caused by the action of paraplow ripper serves as the basis for determining its installation on the implement. Thus, Table and Figure 2 show that both normal and shear stresses in the transverse direction at the distance of 20 cm from the point of force application are minimal and at the distance of 12 - 14 cm they are still significant. Consequently, the

paraplow rippers in transverse directions should be placed at a distance of 24 - 28 cm.

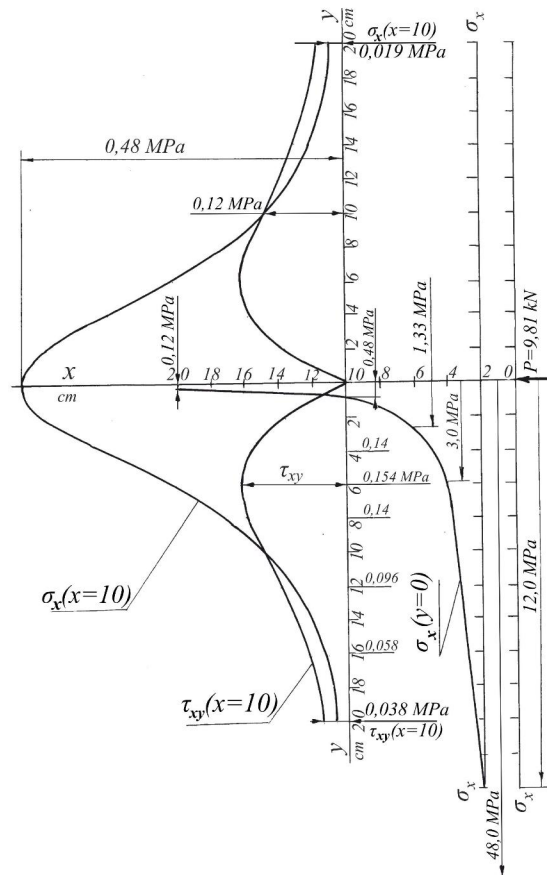


Figure 2. The stress distribution in soil under the effect of paraplow ripper

5. Conclusion

The interaction of the paraplow ripper with soil was examined. Stresses in soil layers under the action of a working body and the nature of their distribution were investigated. Parabolic equations describing the distribution of normal and shear stress in the soil were derived. Their numerical and graphical analysis can solve the problem of the balance of working bodies on the machine's frame. Practical advice for machine designers is presented.

Corresponding Author:

Prof. Dr. Dimitar Karaivanov
Department of Applied Mechanics
University of Chemical Technology and Metallurgy
8 Kl. Ohridski Blvd., 1756 Sofia, Bulgaria
E-mail: dipekabg@yahoo.com

References

1. Broek D. Fundamentals of fracture mechanics. Vysshaya Shkola, Moscow. 1980. (in Russian)
2. Morozov EM, Zernin MV. Contact problems in fracture mechanics. Mashinostroyeniye, Moscow. 1990 (in Russian)
3. Slepyan Slepyan LI. Fracture mechanics. Sudostroeniye, Leningrad. 1990. (in Russian)
4. Pluinage G. Mechanics of elastic-plastic fracture. Mir, Moscow. 1993. (in Russian)
5. Eskhozhin DZ. Theoretical basis of soil mechanics. S.Seifullin KATU Science Review. 2003; V. 3, № 9. – Astana: 144-147.
6. Freud LB, Clifton RJ. On the uniqueness of plane elastodynamic solutions for running cracks. J Elasticity 1974; 4, No.4: 293-299.
7. Williams ML. On the stress distribution at the base of a stationary crack. Trans ASME J Appl Mech 1975; 24: 109-114.
8. Reidel H, Rice JR. Tensile crack in creeping solids. In: Fracture Mechanics. Twelfth Conference ASTM STP 700, 1980: 112-130.
9. Reidel H. Fracture at high temperature. Springer, Berlin. 1987.
10. Freud LB. Dynamic fracture mechanics. Cambridge University Press, Cambridge, 1990.
11. Jun Z, Xing Z. The asymptotic study of fatigue crack growth based on damage mechanics. Eng. Fracture Mechanics 1995; 50, No. 1: 131-141
12. Ferjani at al., 2011 Daniel Averbuch, Andrei Constantinescu. (2011) Semianalytical solution for the stress distribution in notched tubes. // International Journal of Fatigue v.33. pp.557-567.
13. Carrere J, Martinez JE (2013). 3D stress distribution analysis around blind-holes in thin plates under non-uniform tension loads. Int Journal of Engineering Research and Applications 3, 2013: 1017-1022.
14. Dewangan A, Gupta DP, Bakshi RK (2013). Stress distribution analysis of the kaolinite layer at the kaolinite-geotextile. Intl Journal of Innovative Technology and Exploring Engineering. 2013; v. 2: 162-165
15. Gao Z, Zhan J. Evaluation on failure of fibre-reinforced sand. Journal of Geotechnical and Geoenvironmental Engineering 2013; 139, No. 1: 23-31.
16. Ghosh R. Effect of soil moisture in the analysis of undrained shear strength of compacted clayey soil. Journal of Civil Engineering and Construction Technology 2013; 4(1): 23-31.
17. Nukheshev SO. Scientific basis of differentiated subsurface mineral fertilizers application in precision farming system (monograph). Astana. 2011. (in Russian).
18. Vyalov SS. Rheological fundamentals of soil mechanics. Vysshaya Shkola, Moscow.1978. (in Russian).

1/12/2014